

Superhydrophobic ZnO Nanowires: Wettability Mechanisms and Functional Applications

Rasa Mardosaitė, Aušrinė Jurkevičiūtė, and Simas Račkauskas*



Cite This: *Cryst. Growth Des.* 2021, 21, 4765–4779



Read Online

ACCESS |

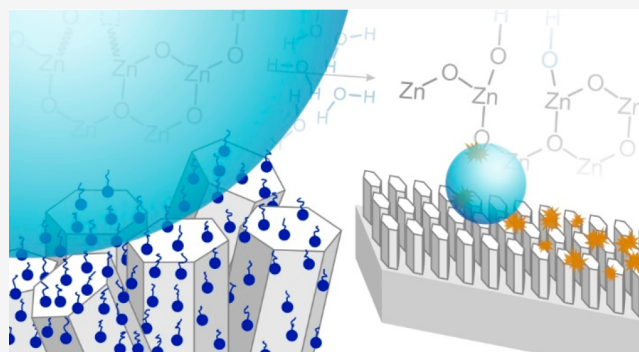


Metrics & More



Article Recommendations

ABSTRACT: Superhydrophobic surfaces are important parts of many applications in cleaning and protective coatings. Such surfaces can be realized by controlling the surface chemistry and nanoscale structure. Elongated ZnO nanostructures, called nanowires, are often used in superhydrophobic applications due to their intrinsic characteristic advantages and simple synthesis control. This review presents a critical overview of the latest research activities focused on the ZnO nanowire superhydrophobic surfaces. A wettability mechanism background is introduced with the overlay of the crystal structure fundamentals adapted for ZnO nanowires to gain insights into the multifunction application of superhydrophobic ZnO nanowires. Moreover, the latest achievements in application of ZnO superhydrophobic nanowires or reversible wettability for self-cleaning, separation, antifogging, antibacterial, and other applications are outlined. Finally, a brief outlook on the issues and emerging perspectives of ZnO nanowire wettability research is summarized.



1. INTRODUCTION

Nanotechnology holds a promise in creating novel materials with desirable and tunable properties. However, still there is a challenge to efficiently control the structure of nanomaterials in order to induce interesting properties. One of the interesting application of nanostructures is surface hydrophobicity control, which can be achieved by playing with the structure and surface chemistry. One-dimensional crystals—nanowires—are especially interesting for wettability control, for the reason that with a perfect manipulation of the height and pitch between nanowires a perfect superhydrophobic structure can be achieved.

ZnO nanowires, also known as nanorods, nanoneedles, nanobelts, or nanowiskers, possess unique structural and functional properties, which makes them advantageous for multifunctional superhydrophobic applications. First, ZnO has three different crystallographic fast grow directions, which makes it possible to synthesize different nanostructures with a growth control. Second, ZnO nanowires are photocatalytic, antibacterial, UV absorptive, biocompatible, transparent and stable in high temperatures, and therefore, multifunctional superhydrophobic surfaces can be obtained. ZnO nanowires are also environmentally friendly as they can be produced from abundant Earth crust materials with low ecological impact. ZnO does not pose a significant threat to organisms and is used as a dietary element and for skin ointments. Last, the functional advantage of ZnO nanowires is the unique reversible switching of wettability, which allows changing the ZnO

nanowire surface from hydrophobic to hydrophilic by manipulation of the atmosphere, heating, or illumination.

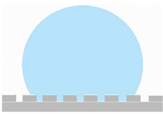
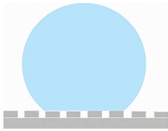
This Review will bring an overview of the latest activities focused on the ZnO nanowire superhydrophobic surface research and application. The review consists of two parts: the first part is devoted to the mechanisms of superhydrophobicity, starting from the fundamentals of wettability and bioinspired models. The mechanism of superhydrophobicity is discussed and adapted for different planes of ZnO nanowires. Further, a hydrophilic–hydrophobic reversible switching mechanism based on oxygen-related surface defects is presented, describing the possibilities to induce and control the change in ZnO nanowire wettability. The second part brings an overview of the progress from recent research on ZnO nanowire-based superhydrophobic materials application for self-cleaning, separation, antifogging, and other fields. ZnO nanowire preparation techniques and functionalization options will be discussed. The Review is concluded with remarks and future outlook, highlighting the current state of knowledge of the ZnO nanowire wettability mechanisms and pointing to the

Received: April 16, 2021

Published: June 30, 2021



Table 1. Comparison of Wenzel and Cassie–Baxter Models

Wenzel's model	Cassie–Baxter's model
	
A liquid drop completely wets a solid rough surface	A liquid drop contacts only the top of roughness on a solid surface
Wetted surface state	Nonwetted surface state
Total liquid penetration with no solid–air interface	Liquid does not penetrate into roughness, liquid–air and liquid–solid interfaces exist
Surface roughness highlights native surface wettability features: roughness makes a hydrophobic surface more hydrophobic while hydrophilic surface more hydrophilic	Surface gets more hydrophobic as the solid fraction decreases
On a rough hydrophobic surface CA hysteresis significantly increases due to the increased contact area between liquid and solid	On a rough hydrophobic surface CA hysteresis decreases due to the reduced contact area between liquid and solid
Lotus leaves Macroscopically smooth leaves contain hierarchically rough surface: microscale bumps covered with wax crystalloids	Lady's Mantle leaves Water drops are lifted from the less hydrophilic cuticula into the brush of more hydrophilic elastic hairs

promising research areas on investigation toward robust superhydrophobic surfaces and multifunctional applications.

2. BIOINSPIRED MODELS OF WETTABILITY

A closer look at biological water-repellent plant leaves reveals at least two types of surfaces that let morning dew or rain drops runoff freely. First of these, Lotus-type leaves contain small scale structures (wax microcrystals) which are responsible for water repellency, whereas the second type of leaves (e.g., Lady's Mantle leaves) have a noticeable hair-covered surface;¹ consequently, two models of surface wettability (Wenzel and Cassie–Baxter) are revealed. Both models describe a water contact angle (CA) increase with increasing surface roughness. However, the theory of Cassie–Baxter characterizes an effect of trapped air pockets within a textured surface that causes a notable increase in CA.^{2,3} In other words, this model predicts that the surface gets more hydrophobic as the solid fraction of contact gets smaller. A brief comparison of Wenzel and Cassie–Baxter models is presented in Table 1.

The water droplet has a very low adhesion to the surface in a Cassie–Baxter regime as it is sitting on the top of the irregular structure with air pockets (e.g., Lady's Mantle leaves have an elastic hair cover). The Wenzel regime involves the stronger adhesion of a water droplet with a surface, as the air pockets are filled with water, and drops are pinned to the solid surface (smooth Lotus leaves contain a hierarchically rough surface).

These two bioinspired regimes provide fundamental principles for the scientific world and engineers to design synthetic superhydrophobic surfaces with a water CA larger than 150°. This CA value of solid surfaces is a benchmark for scientists implementing various synthesis strategies in order to achieve surface nanostructures with desired morphologies and hierarchies. Among others, ZnO nanowires have one of the most pronounced morphologies suitable for superhydrophobic applications because of their crystal structure, controllable height and density, compatibility, and possibility to change the

surface characteristics of textiles and polymers.² Two wettability regimes of substrates covered with hierarchical structures of ZnO nanowires, inspired by the bioregimes,⁴ are presented in Figure 1.

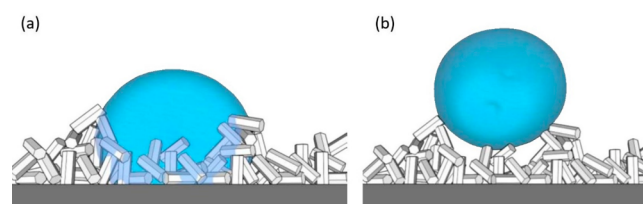


Figure 1. Two wettability regimes on substrates covered with ZnO nanowires: (a) Wenzel regime, (b) Cassie–Baxter regime. Adapted with permission from ref 4. Copyright 2019 Elsevier.

3. ORIGIN OF ZnO NANOWIRE WETTABILITY

The hexagonal wurtzite structure of ZnO has three types of fast growth directions: *c*-plane growth (0002), *m*-plane growth (10 $\bar{1}$ 0), and *a*-plane growth (11 $\bar{2}$ 0).⁵ Because of different surface constructions, polar and nonpolar ZnO surfaces can be achieved via manipulations of ZnO crystallographic orientations and surface engineering. The ZnO wurtzite crystal structure grows along the *c*-axis: layers of Zn/O/Zn/O ions create a sequence in the [0001] direction.⁵ This direction has the fastest growth rate and are most common in ZnO nanowire-based structures. In contrast, nonpolar *m*- and *a*-planes of ZnO crystals are also favorable when the polar plane growth is suppressed with capping agents.^{6,7}

ZnO polar and nonpolar surfaces have different wettabilities. Table 2 provides an overview of wettability data of some ZnO nanostructure surfaces. The ZnO surface wettability relation with the different crystallographic orientations was studied by Wei and co-workers.⁶ The team prepared ZnO thin films with crystallographic orientations from purely polar *c*-plane surfaces

Table 2. Water CA Values for Various Polar and Nonpolar ZnO Surfaces

ZnO structure and surface		orientation	water CA, °	ref
ZnO elongated nanograins	nonpolar	<i>m</i> -, <i>a</i> -plane coexisting ZnO	110.1	6
ZnO elongated nanograins	polar and nonpolar coexisting	<i>c</i> -, <i>m</i> -plane coexisting ZnO	105.49	6
ZnO elongated nanograins	polar	pure <i>c</i> -axis ZnO	113.66	6
ZnO nanorods	nonpolar	not specified	from 112 to 139.6	7
ZnO nanorods	polar	not specified	~0 (after daily measurements ~90)	7
ZnO nanoparticles	polar	<i>c</i> -axis: zinc-terminated [0001]-Zn	29 ± 2	8
ZnO nanoparticles	polar	<i>c</i> -axis: oxygen-terminated [0001]-O	33 ± 2	8
ZnO nanorods	polar	<i>c</i> -axis	74 (after enhanced roughness 131.2)	10
ZnO nanorods	polar	<i>c</i> -axis	9.6 ± 0.8	9

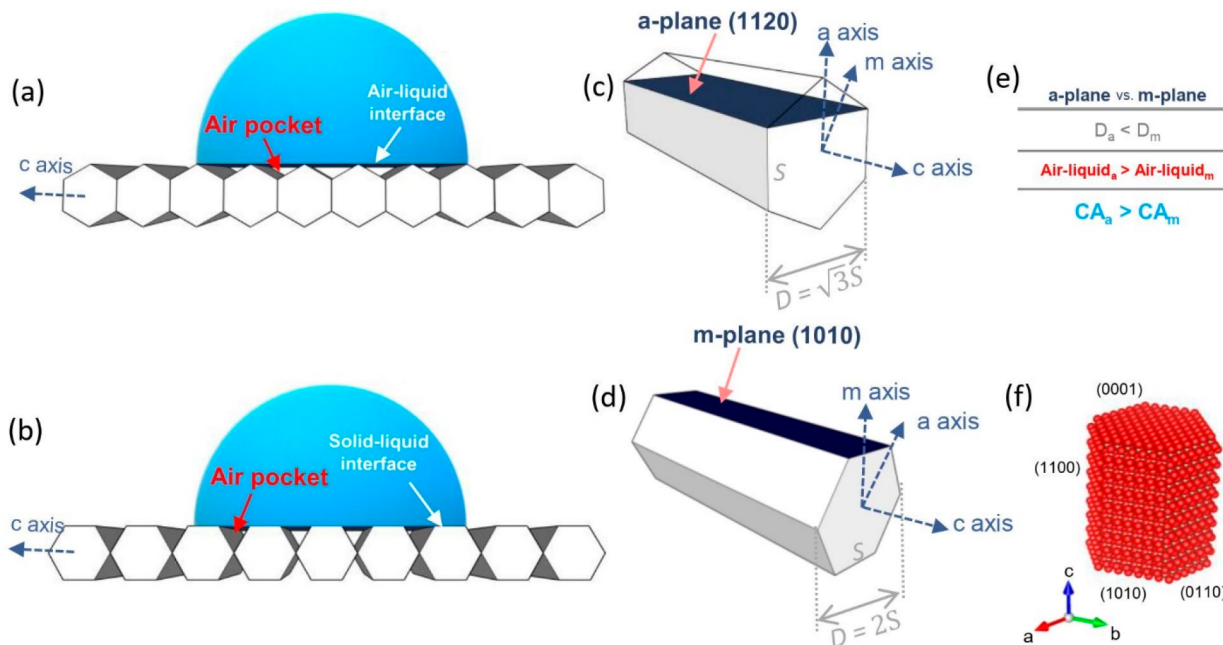


Figure 2. Schematic view of surface wetting on a ZnO nanowire with (a) *a*-plane and (b) *m*-plane nonpolar orientations, (c–e) their wurtzite structures with specified characteristics, and (f) crystal structure of wurtzite ZnO. Adapted with permission from ref 6. Copyright 2016 American Chemical Society.

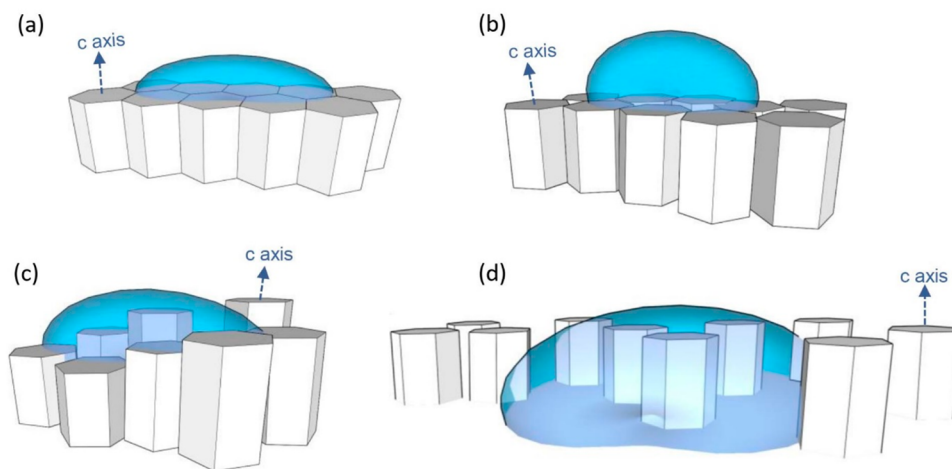


Figure 3. Surface wetting effects on the (a) smooth and (c–d) rough surface of polar *c*-plane-oriented ZnO nanowires; hydrophobicity can be increased by apertures (b) for air pockets, while hydrophilic properties can be obtained by variation of nanowire height (c) and density (d).

to a totally nonpolar oriented *m*-plane, which demonstrated a slight change in water CA. The reasons for such changes are discussed in the following paragraphs for polar and nonpolar ZnO surfaces separately.

3.1. Wettability of Nonpolar ZnO Planes. Figure 2 illustrates how different wettabilities can be achieved on the nonpolar *a*- and *m*- planes of ZnO. In order for a surface to be highly superhydrophobic, water drops must sit on a uniform

layer of trapped air between the water and the surface (i.e., Cassie–Baxter regime¹⁰). Trapped air acts as a physical barrier which can also be observed when the surface is submerged in water due to an optical mirror effect. This effect is provoked due to the total internal reflections of light reflecting off the trapped air layer.³ For the nanowires with *a*- and *m*-plane orientations, the surface of air pockets existing in interstices between *a*-oriented structures (Figure 2a) is higher than that of *m*-oriented structures (Figure 2b).⁶ *S* and *D* are the hexagon side length and the distance between the hexagon sides on the *c*-plane of ZnO nanowire, respectively. This effect can be explained by geometry. The distance of an *a*-plane nanowire $D_{a\text{-plane}}$ is slightly smaller than the $D_{m\text{-plane}}$ (Figure 2c–d). This leads to the increased water–air and lower solid–liquid contact surface (Figure 2e) and consequently enhances the water CA on *a*-plane oriented ZnO surfaces compared to *m*-plane orientations ($CA_a > CA_m$).

3.2. Wettability of Polar ZnO Planes. The nature of an interaction between surface and water drop depends on the orientation of ZnO crystal. Since the influence of *a*- and *m*-nonpolar orientations was already assessed in the previous paragraph, the single-crystalline ZnO nanowires with the *c*-axis perpendicular to the surface can be used as a benchmark to study the wetting process on *c*-axis-oriented ZnO thin films and coatings. Figure 3 illustrates polar single-crystalline *c*-plane oriented ZnO nanowire array wettability, which differs from the nonpolar ZnO surfaces discussed. Intrinsically, the *c*-plane-oriented single-crystalline ZnO surface is hydrophilic: the water CA on the flat surface of a ZnO single crystal is 31°. CA is different for zinc-terminated [0001]-Zn and oxygen-terminated [0001]-O surfaces of the wurtzite crystal structure: 29° ($\pm 2^\circ$) and 33° ($\pm 2^\circ$), respectively.⁸ However, many studies reported various CA values on ZnO nanowires.

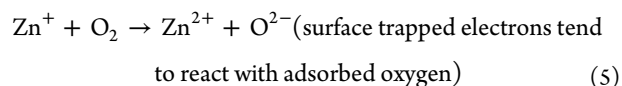
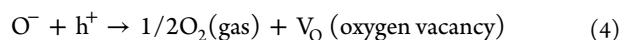
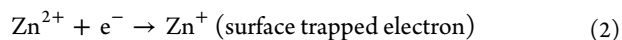
Hydrophobicity of the ZnO nanowire polar surface can be increased by creating air pockets between nanowires. Many authors declare hydrophobic behavior of ZnO nanowires with relatively high water CA up to 157°. CA values around 90° and higher can be connected to formation of apertures between nanowires without distinctly increasing the surface roughness of a flat film surface.¹³ More apertures provide more trapped air which reduces the water–surface contact area as shown in Figure 3b. A minor distance between nonpolar lateral facets of ZnO nanowires generates a strong repulsion charge for these facets.⁷ In this case, the CA value is higher due to the replacement of the flat hydrophilic surface by air pockets having a CA of 180°. However, this effect can be assigned only for flat and smooth surfaces with nanoscale roughness.

A hydrophilic ZnO polar surface with a CA much lower than the intrinsic 31° can be also obtained by changing the ZnO nanowire height and density distribution as shown in Figure 3c–d. According to Wenzel's model,¹⁴ the surface roughness can affect both hydrophobic and hydrophilic features increasing their hydrophobic and hydrophilic properties, respectively.⁹ A water CA of $9.6 \pm 0.8^\circ$ on highly oriented ZnO nanowire array films was measured by Cai et al.⁹ Mallick and co-workers recently reported the water CA of 20.2° for ZnO nanowire-based films prepared by a hydrothermal method.¹⁵ Turmine and co-workers have reported the CA of about 0° of a smooth ZnO layer with polar facets immediately after the hydrothermal synthesis.⁷

4. HYDROPHOBIC–HYDROPHILIC MANIPULATION OF ZNO WETTABILITY

The oxygen-related surface defects are typically responsible for interchange between superhydrophilic and superhydrophobic ZnO states.^{16,17} The light illumination, thermal and chemical treatment effects convert the wettability of ZnO nano-surfaces;¹⁸ thus, understanding of external stimuli-induced reversible wettability is critical for the real-life application of ZnO multifunctional properties.

4.1. Thermal- and Photoinduced Reversible Wettability of ZnO. One of the most common manipulation methods is photoinduced reversible wettability,^{18–20} where the ZnO surface is treated with a light of energy higher than the bandgap. In the latter study, as-synthesized superhydrophilic ZnO nanowires were converted to superhydrophobic surfaces after storage in the dark for several months and returned to a superhydrophilic state by the UV light illumination only for several minutes.¹⁸ The hydroxyl radicals followed the route attached-removed-restored phase on the ZnO surface. The electron–hole pair was generated by illumination with UV of higher energy than the ZnO band gap. The carriers moved to the surface inflicting following reactions: (i) electrons reacted with the lattice metal ions Zn^{2+} forming Zn^+ defective sites, and (ii) the hole reacted with lattice oxygen forming the surface oxygen vacancies. Kinetically favorable hydroxyl (–OH) adsorption from the air moisture is performed on the oxygen vacancies sites. Even though the hydroxyl adsorption reaction is faster, oxygen adsorption is more thermodynamically favored on these oxygen vacancies: oxygen is more strongly bonded on the defect sites than –OH groups. The reversible wettability can be justified here as the initial superhydrophilic nature of ZnO is gradually replaced by superhydrophobic surfaces by –OH removal/oxygen adsorption in the long-term dark storing conditions, while these surfaces can be quickly returned to –OH terminated superhydrophilic states after UV illumination.^{17,19,20} In general, the photoinduced process can be expressed by the path of the following reactions (1–5):²¹



The wettability of ZnO nanowires can be converted by annealing in reducing or oxidizing atmosphere. The heating in [Ar:H; 96:4] at 400 °C results in oxygen vacancy generation in ZnO powders.²² Recently, the superhydrophobicity of the ZnO nanoparticles was switched to the superhydrophilic state along with creation of oxygen vacancies after annealing at 400 °C under ambient atmosphere.²³ Interestingly, the superhydrophobicity was restored by decreasing the annealing temperature to 150 °C, suggesting that a lower temperature is sufficient only to accelerate the elimination rate of the –OH groups, thus converting nanostructures into a superhydrophobic state without creating vacancies.²³ A similar effect is observed by Singh et al.¹⁸ where the initial superhydrophilic

ZnO NWs switched to superhydrophobic after annealing in H_2 at 300 °C for 90 min. Similarly to annealing in air, O_2 annealing (300 °C for 60 min) converted superhydrophobic ZnO NWs into superhydrophilic. Hui et al.²⁴ demonstrated that the tetrapod-like ZnO treating in H_2 or a vacuum, does not considerably change the amount of oxygen vacancies compared to initial contents, suggesting that H_2 is eliminating some oxygen from the surface layer. However, the annealing in O_2 reduced the concentration of oxygen vacancies more than twice: the effect was explained as oxygen incorporation.²⁴

External stimuli of UV light or temperature can break Zn–O bonds on the ZnO surface resulting in oxygen vacancies and dangling bonds generation—typical traps for water. Oxygen vacancy manipulations on the ZnO surface by light illumination and thermal effects are schematically shown in Figure 4. After enrichment of the ZnO surface with –OH groups, this superhydrophilic state can be converted to superhydrophobic by aging in the dark.

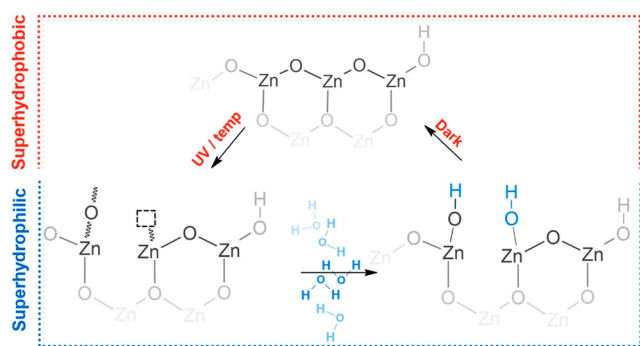


Figure 4. Oxygen vacancies manipulations by light illumination and thermal effects.

4.2. ZnO Surface Wettability Manipulation by Chemical Treatment. Besides the illumination and thermal effects, ZnO surface wettability can be also tailored from hydrophilic to superhydrophobic. The ZnO surface can be plasma treated in order to affect the surface states. For instance, after fluorine plasma treatment on ZnO, fluorine atoms were able to substitute oxygen or occupy oxygen vacancy sites due to similar ionic sizes of fluorine and oxygen.²⁵ As fluorine ions have the strongest electronegativity, in the fluorine-passivated oxide F can attract hydrogen atoms (from ambient air) to bond to the nearest oxygen dangling bond forming intermolecular hydrogen bonds $F \cdots H-O$ and thus an increased amount of hydroxyl groups on the ZnO surface (Figure 5a). As a result, the ZnO surface became more hydrophilic due to passivation of surface vacancies with F. Moreover, F was also incorporated hydrothermally as an anion dopant by Yahaya and co-workers.²⁶ Similarly, a H_2 plasma-treated ZnO surface increased the density of –OH groups and oxygen vacancies (Figure 5b).²⁷

Alternatively, chlorine, as another element of halogens group, was incorporated into the ZnO surface from a simple precursor NaCl leading to increased hydrophilicity.²⁸

ZnO wettability can be altered by depositing a thin layer of other metal oxide. Differently from F and H passivation where hydrophilic properties are increased, the passivation with metal oxide can lead to superhydrophobic behavior. The number of vacancies on the ZnO surface can be decreased due to Zn-dangling bonds passivation by O from Al_2O_3 .²⁷ The effect of

surface defect passivation by a thin Al_2O_3 layer can be understood from the studies of atomic layer deposition (ALD) on the wool surface (Figure 5c),²⁹ which can be related to the surface of ZnO covered with –OH. The increased surface roughness was reported to be a crucial parameter for enhanced fabric superhydrophobicity.

The ZnO superhydrophobic surface can be achieved by ZnO surface defect passivation with surfactants or self-assembled organic molecules.³⁰ Typically, these molecules consist of a long hydrophobic chain of alkyl groups and polar headgroup. The heads are responsible for the connection to the ZnO surface defects, while long alkylic chains will create a rough surface.

A cross-linking reaction between connected molecules induce polymerization or create a network around the surface with reduced free energy and thus increase hydrophobicity. In order to get the well-organized, maximum rough surfactant-enriched surface, precursor selection is critical. For example: after Br occupied oxygen vacancies, surfactants with one long alkyl chain (CPB) create a denser layer than four chains surfactants (TOAB) (Figure 5d) resulting in a more hydrophobic surface.

ZnO defects may be more sensitive to polar protic solvents (Figure 5e). The molecules of such solvents readily donate protons to reagents and thus may provoke hydrophilic ZnO surfaces. It was reported that sonication of ZnO in ethanol or methanol may lead to hydrogen electron passivation of radiative recombination states.^{31,32} Moreover, a range of protic solvents have low separation efficiency for ZnO tetrapods³¹ because of the solvents' low dipole moments.³³ It can be associated with the formation of hydrogen bonds between the H of ethanol and oxygen of the ZnO surface, which can be observed for ZnO nanowires employed as ethanol gas sensors.³⁴

5. SUPERHYDROPHOBIC ZnO NANOWIRE APPLICATIONS

Superhydrophobic ZnO nanowires, needles, or rods have numerous potential applications. Among most common are self-cleaning applications on a superhydrophobic surface, which makes the water roll off easily. Furthermore, superhydrophobicity is useful for the separation of oil and water. Another group of applications is based on the ZnO property to absorb UV light for protection, cleaning, sensing, etc.^{35–37} ZnO is also biologically compatible and thus suitable for biomedical applications. Moreover, for most applications it is important to use Earth-abundant, cheaper, more resistant, and environmentally friendly materials, and ZnO-based devices can meet all of these requirements. In this section, we provide an overview of the most recent applications of superhydrophobic ZnO nanowires. Examples of possible ZnO geometries and water CAs are summarized in Table 3.

5.1. Superhydrophobic ZnO Nanowire Preparation. ZnO nanowires can be synthesized with a variety of techniques by simply controlling the crystal growth direction. Among them, vapor phase and solution phase synthesis can be distinguished.⁴⁸ Vapor phase synthesis involves ZnO nanowire growth by a direct Zn oxidation reaction, whereas Zn salts in aqueous solutions or organic solvents are used for a typical ZnO nanowires solution phase synthesis. The temperature regime for the vapor phase synthesis method is between 400 and 1100 °C, while the temperatures for solution phase synthesis are typically lower than 200 °C.

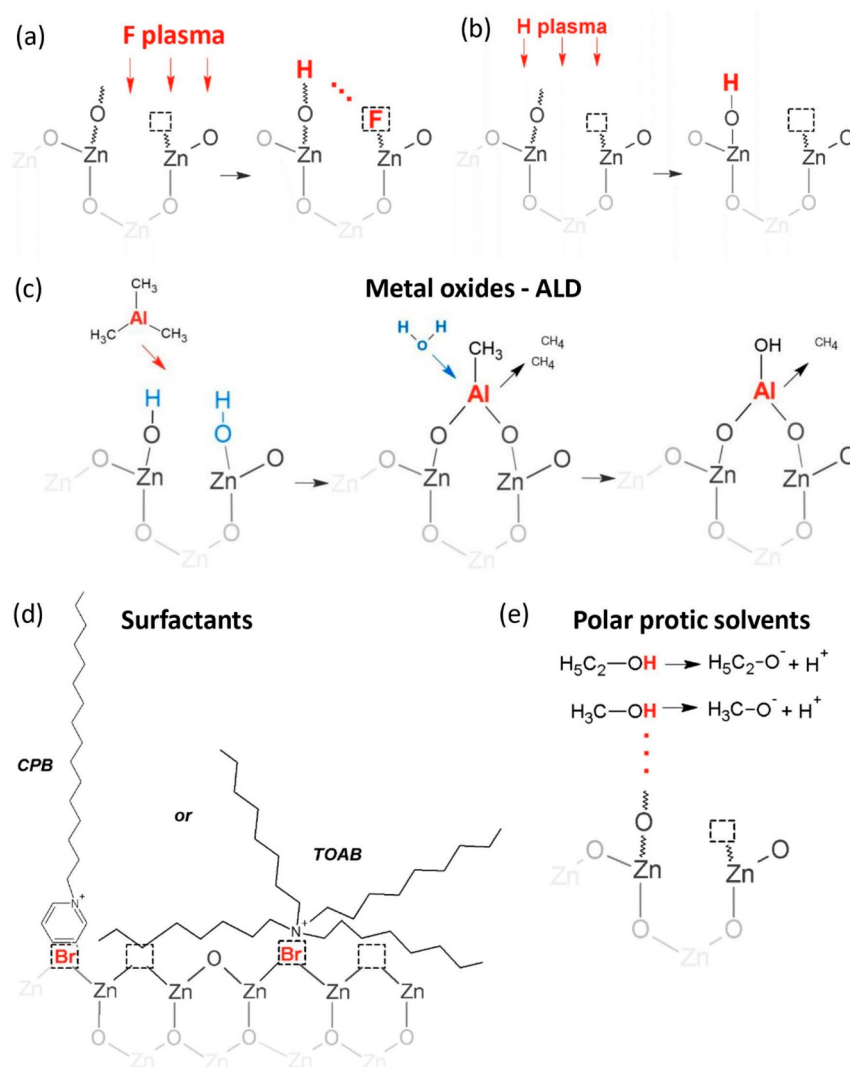


Figure 5. Manipulation of ZnO surface defects: (a, b) passivation by plasma treatment, (c) Al₂O₃ coating, (d) surfactant attachment, and (e) solvation effect.

Table 3. Comparison of ZnO Nanostructures for Different Applications^a

type	synthesis method	size: diameter, nm/length, μm	surface modifications	water CA, $^{\circ}$	application	ref
nanowires, nanorods	hydrothermal	40–60/0.4–1.4	sodium citrate	>90	oil/water separation	38
rods, needles	aerosol-assisted chemical vapor deposition	150–380/1.6	annealing in air	120–134	sensors	37
tetrapods	flame transport	not specified	PDMS	141	wastewater cleaning	39
nanorods	hydrothermal	100–300/3–4	annealing in air/vacuum	146	oil/water separation	40
nanowires	hydrothermal	not specified	POTS	150	antiscaling	41
nanorods	hydrothermal	120/1.5	PFDS	152	water desalination	42
nanowires	thermal chemical vapor deposition	100/not specified	PDMS	153	oil/water separation	43
nanorods	hydrothermal	30–40/0.5–1	silicone	158	antifouling	44
nanorods	hydrothermal	100/2	FAS-17	161	anti-icing	45
nanorods	hydrothermal	100/5	PFDS	162	corrosion resistance	46
nanorods	hydrothermal	300/2.3	F-POSS	164	multifunctional textile	47

^aPDMS – polydimethylsiloxane; POTS – perfluorooctyltriethoxysilane; PFDS – 1H,1H,2H,2H-perfluorodecyltriethoxysilane; FAS-17-heptadecafluorodecyltri-propoxysilane, F-POSS – fluorinated decyl polyhedral oligomeric silsesquioxane.

Wettability of as-prepared ZnO nanowires is not stable. Hydrophobic or hydrophilic properties can be altered due to

the change of temperature, UV, or chemical environment, as it was discussed in section 4. For most applications, initially

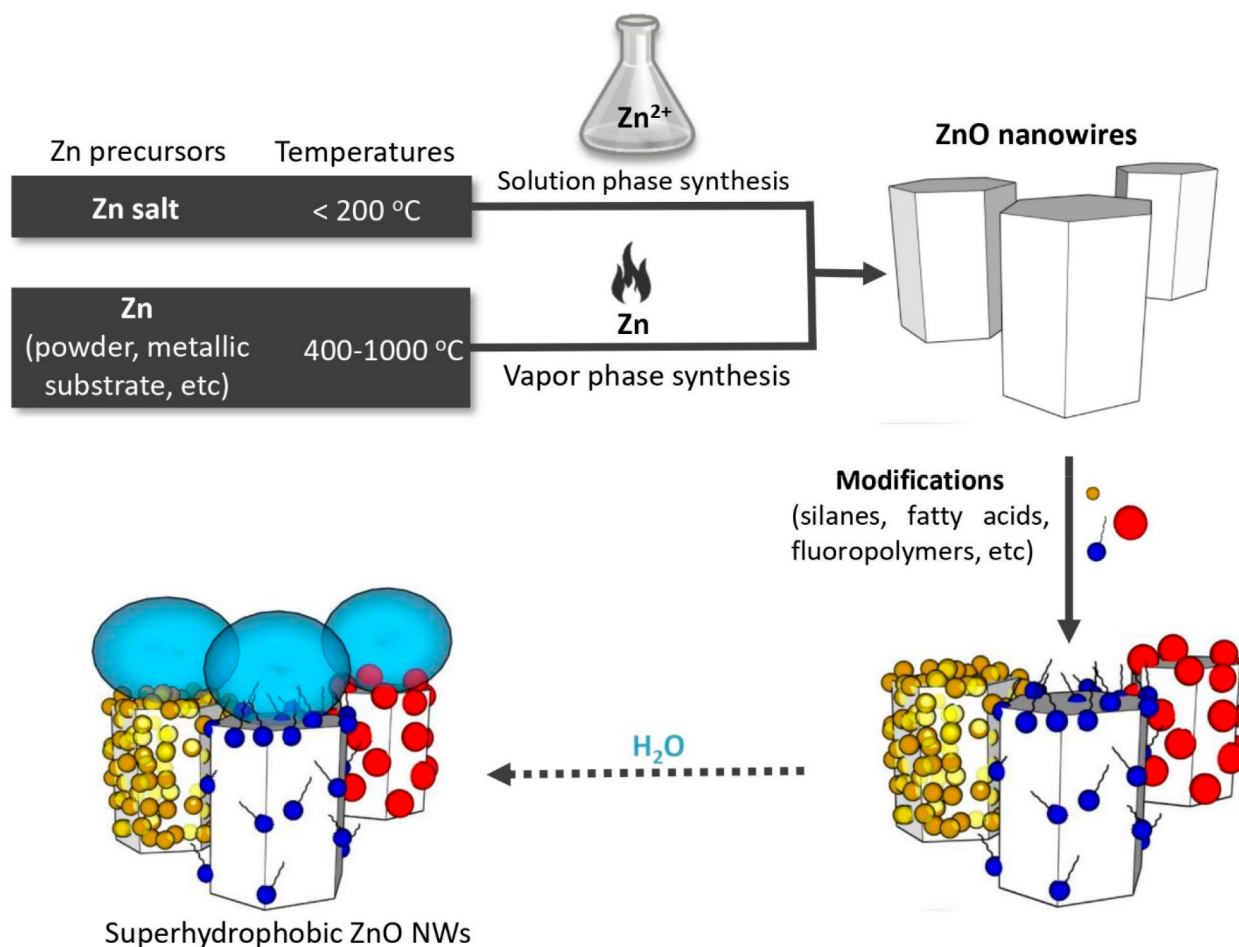


Figure 6. ZnO nanowire synthesis and modification for superhydrophobic application.

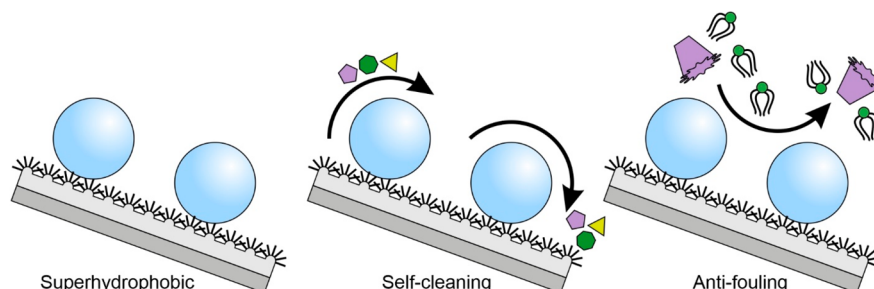


Figure 7. Superhydrophobic ZnO nanowires on polydimethylsiloxane (PDMS) for self-cleaning and antifouling applications. Water forms droplets on superhydrophobic surface, which roll off at low tilt angles along with carrying the pollutants. It also prevents fouling organisms adhering to the surface. Adapted with permission from ref 44. Copyright 2019 Elsevier.

synthesized ZnO nanostructures are additionally modified in order to increase their hydrophobicity.² Most of the reported methods include the surface chemistry modifications with a coating of extreme low surface energy materials such as silanes,⁴⁹ fatty acids,⁵⁰ and fluoropolymers,⁴² resulting in a considerable decrease in surface energy (Figure 6). These ZnO nanowires are typically used to change the surface characteristics of textiles, polymers, and other materials as surfaces with low density will render the surface with relatively high water CA.

5.2. Self-Cleaning Applications. Self-cleaning surfaces would significantly reduce the maintenance cost of solar panels, windows of buildings, aircrafts, etc. In order to obtain

the self-cleaning effect, the surface has to be superhydrophobic (preferably CA of more than 150°), and also the water droplet must slide off the surface at a low ($<10^\circ$) tilt angle.⁵¹ When the water droplet is rolling off the surface, it collects dust or other particulates and thus cleans the surface (Figure 7).⁴⁴

A self-cleaning effect with a water CA of 162° and sliding angle of 4° is achieved on glass, rough silicon, and curved substrates covered with ZnO nanowires grown from the ZnO seed layer containing polystyrene particles.⁵¹ A CA of 154.26° and sliding angle of 5° as well as bouncing of water droplets off the surface are achieved with ZnO tetrapods for dust removal from silicon rubber.⁵² It is possible to achieve sliding angles as

low as 1° , when the glass slide is covered with $\text{Al}_2\text{O}_3/\text{ZnO}$ nanowires.⁵³

The completely water-based functionalization of superhydrophobic ZnO nanowires is possible by spraying with biodegradable fluoroalkylsilane (resulting water CA is 158°). These structures exhibit self-cleaning abilities as the powder from the surface rolls off with the water droplets. The hydrophobic ZnO surface is also antibacterial due to a cushioning effect—the bacteria cannot adhere to the surface.⁵⁴ The surface sprayed with a CuO and ZnO mixture becomes not only self-cleaning (CA = 162.6° , effectively cleans carbon powder) but also corrosion resistant.⁵⁵

ZnO nanowires on PDMS can be employed as an antifouling surface (Figure 7). Because of the superhydrophobicity, pollutants cannot adhere to the surface. The properties are maintained for a long time: after 6 months' immersion in seawater the surface remains clean.⁴⁴ Alternatively, ZnO nanowires can be used as fillers in a PDMS matrix, where ZnO tetrapods fillers show not only the increase in water CA but also in elastic modulus of the composite.⁵⁶

5.3. Water Cleaning and Oil/Water Separation. Fresh water is essential for human well-being, but the resources are limited. Thus, methods for separation of drinkable water from contaminated water are highly desirable. For example, there is plenty of saltwater, and the ability to separate salt and water would be beneficial. More efficient wastewater cleaning, including oils separation, is also an option.

Because of photocatalytic activity, ZnO is suitable for wastewater treatment: the pollutants can be decomposed into less harmful species. It was reported that in 4 h of UV radiation more than 70% of methylene blue and 32% of phenol can be decomposed using ZnO nanowires grown from a 3 nm thick seed layer.⁵⁷ Some complicated structures are suggested for oil adsorption from wastewater; e.g., ZnO tetrapods covered with Fe_2O_3 nanowires are a magnetic sorbent capable of adsorbing 96% of diesel in water with an adsorption capacity of 1135 mg/g.³⁹

Human hair can also work as a water decontaminating agent if functionalized by a 400–600 nm length of ZnO nanowires. Already hydrophobic (water CA 104°) hair after functionalization becomes superhydrophobic (water CA 149°).⁵⁸ Such a composite can photodecompose toxic dyes multiple times with almost the same efficiency. ZnO nanowires attached to human hair are less likely to be released to the environment avoiding the possible toxicity of nanoparticles. In order to degrade the dyes (Methylene Blue, Direct Red 23, Alizarin Red S) or organics (toluene), human hair with ZnO nanowires must be stirred in the solution and irradiated by UV light.⁵⁸ In addition, Methylene Blue can be degraded by using ZnO coated with a zeolitic-imidazolate framework-8.⁵⁹ Dyes (80% of Reactive Yellow 145, 86% of Basic Violet 3) can also be degraded, and heavy metal ions (99% of chromium(VI), 97% of lead(II)) can be removed from water using a ZnO tetrapods nanocomposite with CuO.⁶⁰ Another option for dye degradation is ZnO nanowires modified by fly ash, which are capable of degrading 98% of Reactive Orange 4, 99% of Rhodamine B, and 96% of Trypan Blue in 90 min under natural UV irradiation.⁶¹

Water desalination is possible using a vacuum membrane distillation method, where the poly(vinylidene fluoride) membrane is covered with ZnO nanowires modified by 1H,1H,2H,2H-perfluorodecyltriethoxysilane (PFDS), which leads to better separation efficiency compared to a bare membrane.⁴² When the same type of membrane is coated by

fluorinated ZnO nanowires, the salt separation efficiency is 99.9% with a flux of 15.7 L/hm^2 .⁴¹

ZnO nanowires can be grown on cotton fabric, turning it hydrophobic and oleophobic after treatment with silane coupling agents TTOP-12 or KH550, where water CA is 156° after adding 1.5 wt % TTOP-12 to ZnO precursor.⁶² When the fabric is treated with 2 wt % KH550 in ZnO precursor, it becomes hydrophilic in air but hydrophobic in oil and oleophobic in water with CAs 156° and 157° , respectively.⁶² If the fabric is superhydrophobic and oleophilic at the same time, it can be applied for separation of a water and oil mixture with an efficiency of at least 95%: oil is transmitted due to gravity, and water is kept from transmitting due to hydrophobicity.⁶²

Copper meshes with ZnO nanostructures (nanowires, nanorods, nanosheets) can be made hydrophobic in air but superoleophobic in water (CAs 155° , 153° , 151° , respectively).³⁸ This forms a membrane capable of separating oil from water with 99% efficiency. The efficiency is maintained even after 15 filtration cycles and changes very little when immersed in alkaline, acidic, or salt solutions. The schematics of the separation mechanism are illustrated in Figure 8.³⁸ A

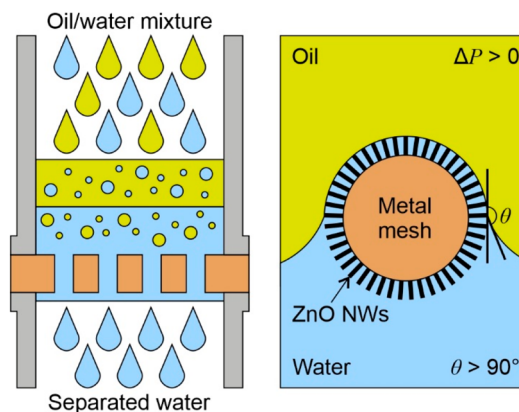


Figure 8. ZnO nanowire-coated metal mesh for oil/water separation based on Cassie theory. Water is trapped in between ZnO nanowires (NWs), which allows water to penetrate the membrane and traps oil on top of it. Adapted with permission from ref 38. Copyright 2019 Elsevier.

stainless steel mesh can also be used instead of copper as a base for ZnO nanowires for water/oil separation. As deposited, the mesh is superhydrophilic in air and superoleophobic in water and lets water permeate through.⁶³ Two-step chemical bath deposition of ZnO micro-/nanohierarchical structures can be used as another option for a stainless steel mesh to become superhydrophobic/superoleophilic for oil/water separation (99.9% efficiency) avoiding low surface energy materials.⁶⁴

ZnO nanowires on a stainless steel mesh can be selectively switched between two modes—oil-removing and water-removing (Figure 9)—by chemical treatment or annealing. The switchable wettability can be realized by treating the ZnO nanowire-coated mesh with stearic acid or NaOH. Stearic acid makes the mesh superhydrophobic (CA $> 150^\circ$) and superoleophilic (CA $\approx 0^\circ$), while NaOH makes it superhydrophilic (CA $\sim 0^\circ$) and underwater superoleophobic (CA $> 150^\circ$); each process of switching takes 15 min. Water/oil emulsion separation is achieved with 99% efficiency, which barely decreases after eight separation cycles.⁶⁵

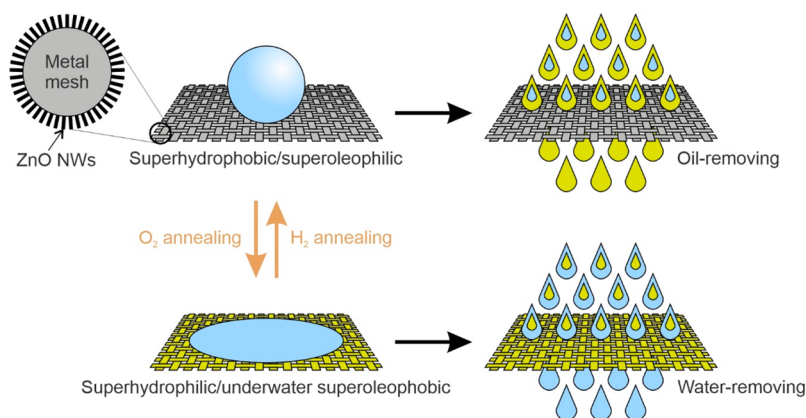


Figure 9. Switchable wettability schematics of metal mesh with ZnO nanowires for oil or water removal. O_2 annealing makes the surface superhydrophilic/underwater superoleophobic, while H_2 annealing reverses the surface back to a superhydrophobic/superoleophilic state. Adapted with permission from ref 43. Copyright 2017 American Chemical Society.

The wettability of ZnO nanowires on a stainless steel mesh can also be switched by annealing in poly(dimethyl siloxane) vapor at 210 °C for 20 min (oil blocking state) and in air at 300 °C for 25 min (water blocking state).⁴³ Alternatively, a similar structure becomes superhydrophobic by annealing in hydrogen atmosphere at 300 °C, which can be reversed to hydrophilic in oxygen atmosphere, leading to a separation efficiency of 99.9% even after 10 cycles of use.⁶³

A carbon fiber membrane can also be coated with ZnO nanowires for oil/water separation. The switchable wettability is achieved by annealing in either a vacuum or air gas atmosphere. Even after five cycles, the switchability is maintained with the same efficiency. Heptane, diesel, chlorobenzene, toluene, etc. were removed from water with a 98–99.5% efficiency, which is maintained for 15 cycles.⁴⁰ Another promising structure for oil/water separation is a polyethersulfone membrane with ZnO rods, fabricated without the use of harmful modification agents.⁶⁶

ZnO nanoneedles arranged in flower-like structures are initially superhydrophobic ($\text{CA} = 163.8^\circ$) but can be turned superhydrophilic ($\text{CA} \approx 0^\circ$) by annealing in ambient atmosphere at 400 °C for 30 min. The superhydrophobic effect is reversed after another annealing in ambient atmosphere at 150 °C for 2 h. These structures show excellent durability in water: superhydrophobicity is maintained even after 12 h of immersion. When ZnO nanoneedles are formed on cotton or metal meshes, they can be used for chloroform/water separation with 97% efficiency, which drops the efficiency to 91% after 10 cycles (Figure 10).²³

5.4. Antifogging and Anti-Icing Application. Superhydrophobicity of ZnO nanowires can be maintained even at temperatures below 0 °C. The water droplet cannot attach to the surface at temperatures below zero degrees; therefore, the ice or frost also cannot be formed—the process is called icephobicity. At -10 °C and -20 °C temperatures, condensed droplets can roll off the surface.⁴⁵ It is reported that ZnO nanowires can maintain some level of icephobicity at temperatures down to -150 °C.⁶⁷

Superhydrophobic ZnO nanowires sputtered by a radio frequency magnetron method can delay frosting of the entire surface for 140 min at -10 °C or for 153 min at -5 °C. Even after 30 cycles of frosting and defrosting, ZnO nanowires do not show observable damage, thus indicating an excellent durability. During the defrosting process, the sample was tilted

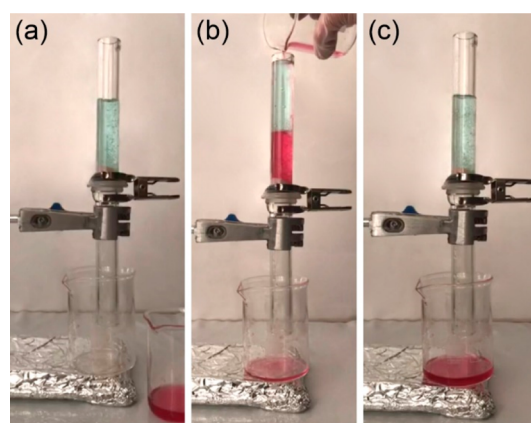


Figure 10. Separation process of chloroform (pink) and water (blue) using ZnO: (a) a glass tube filled with water before the separation process, (b) pouring of chloroform into the tube with water, (c) chloroform penetrates the membranes and is collected in the beaker, while water is cleaned and stays in the tube. Reprinted in part with permission from ref 23. Copyright 2018 Elsevier.

at 15°, which allows the meltwater to roll off the surface in such a way leaving it dry for subsequent frosting cycles. At 0°, complete fogging of the surface is avoided as water forms droplets, which can be easily blown off.⁶⁸ After 15 min of ZnO radio frequency magnetron sputtering on Al, the surface does not freeze for 2 h and is not covered in frost for 5 h at -10 °C.⁶⁹

The ability of the surface to avoid frosting depends on the amount of air in the surface morphology. It was reported that for a stainless steel surface with fluorinated circular holes and ZnO nanowires around them, substrate frosting is delayed by 63 h at -21 °C and 75% humidity, compared to just 3 h for a bare stainless steel substrate.⁷⁰ A surface with anti-icing properties can also be obtained by covering it with multi-layered, needle-like structure, which includes ZnO, SiO_2 , and polytetrafluoroethylene. In such case, after 2 h of spraying ice on the substrate only 17.9% of the surface gets covered in ice.⁷¹

5.5. Multifunctional Applications. 5.5.1. Biomedical Applications. Wettability properties are very important when considering materials for implants. Hydrophobic surfaces can prevent diseases caused by bacteria found in water. ZnO nanowires on a silicon surface can be superhydrophobic, which can also help to increase the CA of blood on various surfaces:

from 54.6° to 96.4° on quartz, from 28.5° to 145.7° on glass, from 62.0° to 138.8° on silicon, and from 81.4° to 131.6° on PDMS.⁷² Moreover, ZnO also has antibacterial properties (killing bacteria under UV irradiation), which makes it a good choice for biomedical applications.⁷²

It was proven that ZnO nanoneedles have antibacterial properties against *Staphylococcus aureus*, *Staphylococcus epidermidis*, *Streptococcus pyogenes*, *Escherichia coli*, *Pseudomonas aeruginosa*, *Serratia marcescens*, and *Klebsiella pneumonia* (the inhibition zone is 12–18 mm depending on the bacteria when ZnO is dissolved in dimethyl sulfoxide).⁷³ Nevertheless, the antibacterial effect is slightly better in the case of ZnO nanosheets and nanodrums; the inhibition zone is on average 15% larger than in the ZnO nanoneedles case (however, the differences in hydrophobicity are not reported).⁷³ ZnO nanowires covered in Ag nanoparticles are also reported to have an antibacterial effect for cotton fabric against *Staphylococcus aureus* and *Escherichia coli*.⁷⁴ Ce-doped ZnO has antibacterial properties against *Staphylococcus aureus* with a rate of 83%. Against *Escherichia coli*, cotton fabric has better antibacterial activity when covered with ZnO without Ce doping (83%).⁷⁵ Several ZnO antibacterial mechanisms have been suggested (Figure 11a): (1) induction of oxidative stress through reactive oxygen species, which leads to cell damage or death; (2) release of Zn²⁺ inhibits cell activities, e.g., active transport, bacteria metabolism, enzymes activity; (3) ZnO attachment to the cell membrane through electrostatic forces, which distorts the membrane plasma structure and damages the cell integrity.⁷⁶

ZnO is biocompatible and is thus a promising material for biosensors. Moreover, ZnO nanowires in the shape of tetrapods are more biocompatible compared to their spherical counterparts.⁷⁸ ZnO nanowires of 200 nm diameter and several micrometers in length on a silicon substrate were tested as an optical sensor for grapevine virus A-type: the defect-related photoluminescence spectrum experiences a shift up to 5 nm. However, the superhydrophobicity of ZnO nanowires can reduce the sensitivity of the sensor, and thus the hydrophobicity is intentionally decreased by UV irradiation.⁷⁹ Since ZnO nanostructures can be easily deposited on flexible substrates, such as fabric, they are interesting for applications in noninvasive, wearable sensors for real-time monitoring. For example, cortisol in human sweat is detected by ZnO nanowires synthesized on flexible carbon yarns.⁸⁰

Lab-on-a-chip is another interesting field of possible applications of ZnO nanowires. With a decreasing size of channels in lab-on-a-chip, the liquid flow resistance increases, especially for smooth hydrophilic surfaces. ZnO nanowires help to maintain a constant flow of liquid in a device independently of surface wetting properties.⁸¹

5.5.2. Functional Coatings. ZnO nanostructures have UV blocking capabilities with a tunable peak position depending on the thickness and annealing temperature;⁸² therefore, they are often used in UV filters or sunscreens.^{83–85} Films of ZnO particles can be reshaped into nanorods by annealing at 180 °C, which increases their ability to absorb up to 50% of UV light while maintaining more than 80% transmission in the visible spectrum.⁸² By incorporating MXenes and Ni-chain into the coating with ZnO nanowires on cotton fabric, enhanced microwaves absorption can be achieved (compared to nonmodified ZnO).⁴⁷ Such a modification also allows for the fabric to be superhydrophobic to various liquids (Figure 11b).

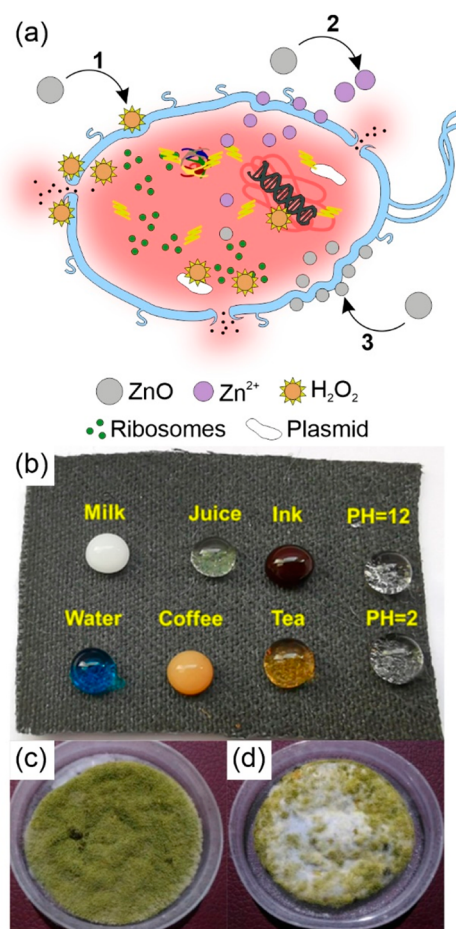


Figure 11. (a) Schematic of the antimicrobial mechanism of ZnO against the bacterial cell: (1) formation of reactive oxygen species, (2) dissolution of ZnO into Zn²⁺, (3) direct interaction between ZnO and the cell membrane. Adapted from ref 76 (Creative Commons CC BY). (b) Digital camera image of various liquids on ZnO nanowire-based nanocomposite coated fabric. Reprinted with permission from ref 47. Copyright 2020 American Chemical Society. Growth of fungus on dough after 5 days: (c) bare dough, (d) dough coated with 20% Ce-doped ZnO. Reprinted with permission from ref 77. Copyright 2019 Elsevier.

ZnO nanowires can also give rise to multifunctional paint coatings, such as cashew nut shell liquid (CNSL) organic base. Adding 10% volume fraction of ZnO nanowires shows multiple advantages: pure CNSL coatings are prominent to cracking, however, ZnO nanowires solve this problem due to binding effects related to intrinsic ZnO morphology. When such a composite (CNSL + ZnO) coating is applied on glass, the water CA increases, and at the same time, the reflectance in the near-infrared region also increases to more than 30% (compared to 3% for pure glass).⁸⁶ When CNSL + ZnO is applied to an AZ31 magnesium alloy surface, it is effectively protected from corrosion: corrosion resistance is increased by 156%.⁸⁶

Coalescence-induced droplets jumping can explain anti-corrosive properties of superhydrophobic films: a layer of liquid on the surface leading to faster corrosion can be ejected by such coating, composed of ZnO nanoneedles.⁸⁷ Better corrosion resistance is achieved by superhydrophobic ZnO nanowires (100 nm diameter, 5 μm length, CA = 161.7°) compared to microrods (800 nm diameter, 10 μm length, CA

= 155.6°).⁴⁶ In addition, a steel substrate can be protected from corrosion by a PDMS/graphene oxide/ZnO nanowires nanocomposite film.⁸⁸

5.5.3. Antifungal Applications. ZnO can also effectively reduce the growth of fungus due to reduced humidity on the hydrophobic surfaces. ZnO nanowires mixed with shellac preserves the wood from a significant change in color due to UV blocking and is more resistant to molding due to hydrophobic properties of the mixture. Shellac is commonly used for wood treatment and ZnO additionally improves the properties. Untreated wood has a CA of 56°, which increases up to 95° after treatment with a ZnO shellac mixture. Untreated wood and wood with shellac both exhibit fungi growth after 2 days in a high humidity environment. However, wood with ZnO does not acquire any fungi even after 40 days in a humid environment. Untreated wood and wood with shellac coating appear darker and more yellow after UV irradiation. By including ZnO into the mixture, the wood is still affected by UV, but the color change is less drastic.⁸⁹

ZnO doped with carbon is another ZnO-based composite for antifungal coatings. When C-doping is performed by thermal deposition, ZnO structures become shaped as nanowires (20% C results in 37 nm size rods), which increases the CA up to 98.4°.⁷⁷ It was reported that such a ZnO:C coating significantly reduced fungus (*Rhizopus Stolonifer*) growth on white flour dough (Figure 11c) compared to both the bare dough and the dough covered with undoped ZnO.⁷⁷ ZnO nanowires on cotton fabric doped with 2.5% of cerium also have antifungal properties against *Candida albicans* with a rate of 85%.⁷⁵

Most structures with antibacterial properties at the same time have antifungal properties. For example, ZnO nanowire and Ag nanoparticle nanocomposites on cotton fabric reduce the growth rate of fungi *Candida albicans* and *Aspergillus flavus*.⁷⁴

5.6. Other Applications. ZnO nanowires have low optical transmission, high absorbance, and reflection and therefore can be applied in optoelectronics and photovoltaics by tuning the band gap energy value, which is related to the morphology of the film.⁹⁰ For example, when ZnO nanowires are used as an electron transport layer, WO₃ as a hole transport layer, and GaIn as an electrode, the photovoltaic device can reach a power conversion efficiency of 4.5%.⁹¹

ZnO nanostructures find their niche application in wearable thermoelectric power generators, which produce electricity from energy in the environment. Even small amounts of energy radiated, e.g., from the human body, can be harvested by creating wearable devices; however, wearable generators have to be superhydrophobic, protected from the UV light, efficient, and nontoxic for the skin. Thus, ZnO is a promising material. By coating the fabric with ZnO nanowires, the water CA increases to 132.5°, and the UV protection factor (UPF) is increased to 116.35. Even better UPF (183.84) is achieved by a mixture of ZnO nanowires (200–400 nm diameter) and nanosheets (4 nm thickness); however, it has a slightly smaller CA (122.4°). ZnO nanowires on textiles have a power factor of 13 $\mu\text{W}/\text{mK}^2$, while nanowires with nanosheets have a value of 22 $\mu\text{W}/\text{mK}^2$.⁹²

ZnO nanowires or nanoneedles without any additives can be used in gas sensors for better performance in a humid environment. The sensor response (the ratio of resistance in air and resistance after 600 s in analyte, i.e., H₂ or CO; Figure 12) is better in the case of ZnO nanoneedles due to a higher

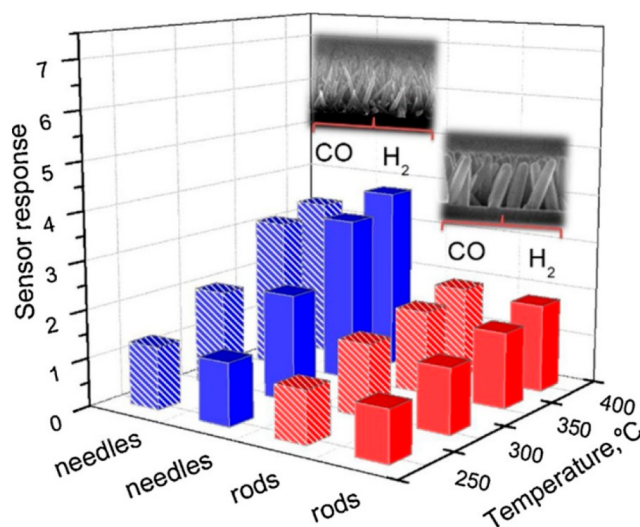


Figure 12. Response of ZnO needle- (left, blue) and rod-based (right, red) sensor for CO and H₂ gases depending on the operation temperature. Reprinted with permission from ref 37. Copyright 2019 Elsevier.

surface to volume ratio. In a humid environment, the response is up to 22% lower.³⁷ Another option for CO gas sensing is growing ZnO nanowires on graphene on cotton fabric.⁹³ Other gases, such as acetaldehyde, ammonia, and ethanol can also be detected by a sensor based on ZnO-functionalized cotton fabric.⁹⁴

ZnO nanowires can be used in UV photodetectors. 420 nm diameter and 6.17 μm ZnO nanowires on indium tin oxide substrate exhibit sensitivity to UV of 2348, while the signal-to-noise ratio is 67 dB.⁹⁵ The sensitivity of 3172.8 to 380 nm wavelength can be achieved in ZnO nanowires using a modified chemical bath deposition technique by introducing air bubbles.⁹⁶ In order to create flexible and effective UV photodetectors, ZnO nanowires can be doped with Cu, Ni/Cu, Co, or Co/Ni, which increases the responsivity.^{97,98} The photoluminescence of ZnO nanowires-based UV photodetector can be increased 6-fold by applying Ag nanoparticles with a SnO₂ shell.⁹⁹ However, metal-doped ZnO-based photodetectors might have compatibility issues in relation to high doping and mobility. This problem can be overcome by introducing graphene as an active layer in ZnO nanowires and GaN heterojunctions.¹⁰⁰ Furthermore, CuO nanostructures can be used in between ZnO nanowires and a GaN layer for UV photodetection at 365 nm wavelength.¹⁰¹ ZnO nanowires are potential materials for switchable dual-response UV photodetectors: in direct current, ZnO nanowires have positive photoconductivity, while in alternating current, the photoconductivity can be either positive or negative, depending on the frequency, which allows fine tuning of the polarity of changes in light and dark resistance.¹⁰²

6. CONCLUDING REMARKS AND OUTLOOK

In summary, superhydrophobic surfaces offer great advantages. A number of techniques are already available for preparation of functional coatings, and applications in various fields are growing. ZnO nanowires have similarities to other nanostructures, used for superhydrophobic applications; however, some special ZnO properties, such as surface defect induction under UV, leads to unique abilities of reversible wettability switching.

Intrinsic characteristic advantages of ZnO nanowires, such as photocatalytic, antibacterial, or antifungal properties can lead to multifunctional superhydrophobic surface applications. More future applications can be envisioned.

Different crystallographic orientations of ZnO nanowires have various wettabilities; however, the distribution, how much space between nanowires for imbedding of air pockets, or the nanowire height and density on the surface are more important, especially if the ZnO nanowire surface is further modified. Oxygen-related surface defects determine the ZnO surface wettability. ZnO nanowire surface reversible switching from superhydrophobic to superhydrophilic controlled by defects can be manipulated by thermal, photoinduced, or chemical treatment, and such effects find application in water cleaning and separation.

However, superhydrophobic ZnO nanowire coatings have some intrinsic problems, which are also characteristic to other superhydrophobic coatings. Nanowire and some other nanostructure based coatings are often brittle, and their superhydrophobic properties deteriorate at high pressure or impact, limiting their practical application. More research should be done in order to find a route for the synthesis of robust superhydrophobic coatings. More effort could also be directed to research on hierarchical superhydrophobic structures, which can be effectively synthesized using ZnO nanowires. Good results and applications can be envisioned.

AUTHOR INFORMATION

Corresponding Author

Simas Račkauskas – Department of Physics, Kaunas University of Technology, LT-51368 Kaunas, Lithuania; Institute of Materials Science of Kaunas University of Technology, LT-51423 Kaunas, Lithuania; orcid.org/0000-0002-8964-5299; Email: simas.rackauskas@ktu.lt

Authors

Rasa Mardosaitė – Department of Physics, Kaunas University of Technology, LT-51368 Kaunas, Lithuania
Ausrinė Jurkevičiūtė – Institute of Materials Science of Kaunas University of Technology, LT-51423 Kaunas, Lithuania; orcid.org/0000-0002-8115-5295

Complete contact information is available at:
<https://pubs.acs.org/10.1021/acs.cgd.1c00449>

Funding

This project has received funding from the European Regional Development Fund (Project No. 01.2.2-LMT-K-718-02-0011) under a grant agreement with the Research Council of Lithuania (LMTLT).

Notes

The authors declare no competing financial interest.

ABBREVIATIONS

CA, contact angle; CNSL, cashew nut shell liquid; FAS-17, heptadeca fluorodecyltri-propoxysilane; NW, nanowire; PDMS, polydimethylsiloxane; PFDS, 1H,1H,2H,2H-perfluorodecyltriethoxysilan; POTS, perfluorooctyltriethoxysilane; UV, ultraviolet

REFERENCES

(1) Otten, A.; Herminghaus, S. How Plants Keep Dry: A Physicist's Point of View. *Langmuir* **2004**, *20* (6), 2405–2408.

(2) Wu, J.; Chen, J.; Xia, J.; Lei, W.; Wang, B. A Brief Review on Bioinspired ZnO Superhydrophobic Surfaces: Theory, Synthesis, and Applications. *Adv. Mater. Sci. Eng.* **2013**, *2013*, 232681.

(3) Simpson, J. T.; Hunter, S. R.; Aytug, T. Superhydrophobic Materials and Coatings: A Review. *Rep. Prog. Phys.* **2015**, *78* (8), 086501.

(4) Mendoza, A. I.; Moriana, R.; Hillborg, H.; Strömberg, E. Superhydrophobic Zinc Oxide/Silicone Rubber Nanocomposite Surfaces. *Surfaces and Interfaces* **2019**, *14*, 146–157.

(5) Mishra, Y. K.; Modi, G.; Cretu, V.; Postica, V.; Lupan, O.; Reimer, T.; Paulowicz, L.; Hrkac, V.; Benecke, W.; Kienle, L. Direct Growth of Freestanding ZnO Tetrapod Networks for Multifunctional Applications in Photocatalysis, UV Photodetection, and Gas Sensing. *ACS Appl. Mater. Interfaces* **2015**, *7*, 14303.

(6) Chao, C. H.; Chi, P. W.; Wei, D. H. Investigations on the Crystallographic Orientation Induced Surface Morphology Evolution of ZnO Thin Films and Their Wettability and Conductivity. *J. Phys. Chem. C* **2016**, *120* (15), 8210–8219.

(7) Ghannam, H.; Chahboun, A.; Turmine, M. Wettability of Zinc Oxide Nanorod Surfaces. *RSC Adv.* **2019**, *9* (65), 38289–38297.

(8) Pesika, N. S.; Hu, Z.; Stebe, K. J.; Searson, P. C. Quenching of Growth of ZnO Nanoparticles by Adsorption of Octanethiol. *J. Phys. Chem. B* **2002**, *106* (28), 6985–6990.

(9) Guo, M.; Diao, P.; Cai, S. Highly Hydrophilic and Superhydrophobic ZnO Nanorod Array Films. *Thin Solid Films* **2007**, *515* (18), 7162–7166.

(10) Cassie, A. B. D.; Baxter, S. Wettability of Porous Surfaces. *Trans. Faraday Soc.* **1944**, *40*, 546–551.

(11) Li, Q.; Cheng, K.; Weng, W.; Song, C.; Du, P.; Shen, G.; Han, G. Room-Temperature Nonequilibrium Growth of Controllable ZnO Nanorod Arrays. *Nanoscale Res. Lett.* **2011**, *6*, 477.

(12) Ennaceri, H.; Wang, L.; Erfurt, D.; Riedel, W.; Mangalgi, G.; Khaldoun, A.; El Kenz, A.; Benyoussef, A.; Ennaoui, A. Water-Resistant Surfaces Using Zinc Oxide Structured Nanorod Arrays with Switchable Wetting Property. *Surf. Coat. Technol.* **2016**, *299*, 169–176.

(13) Chi, P. W.; Su, C. W.; Jhuo, B. H.; Wei, D. H. Photoirradiation Caused Controllable Wettability Switching of Sputtered Highly Aligned C-Axis-Oriented Zinc Oxide Columnar Films. *Int. J. Photoenergy* **2014**, *2014*, 765209.

(14) Wenzel, R. N. Resistance of Solid Surfaces to Wetting by Water. *Ind. Eng. Chem.* **1936**, *28* (8), 988–994.

(15) Nundy, S.; Ghosh, A.; Mallick, T. K. Hydrophilic and Superhydrophilic Self-Cleaning Coatings by Morphologically Varying ZnO Microstructures for Photovoltaic and Glazing Applications. *ACS Omega* **2020**, *5* (2), 1033–1039.

(16) Li, J.; Sun, Q.; Han, S.; Wang, J.; Wang, Z.; Jin, C. Reversibly Light-Switchable Wettability between Superhydrophobicity and Superhydrophilicity of Hybrid ZnO/Bamboo Surfaces via Alternation of UV Irradiation and Dark Storage. *Prog. Org. Coat.* **2015**, *87*, 155–160.

(17) Hu, H.; Ji, H. F.; Sun, Y. The Effect of Oxygen Vacancies on Water Wettability of a ZnO Surface. *Phys. Chem. Chem. Phys.* **2013**, *15* (39), 16557–16565.

(18) Yadav, K.; Mehta, B. R.; Bhattacharya, S.; Singh, J. P. A Fast and Effective Approach for Reversible Wetting-Dewetting Transitions on ZnO Nanowires. *Sci. Rep.* **2016**, *6*, 35073.

(19) Feng, X.; Feng, L.; Jin, M.; Zhai, J.; Jiang, L.; Zhu, D. Reversible Super-Hydrophobicity to Super-Hydrophilicity Transition of Aligned ZnO Nanorod Films. *J. Am. Chem. Soc.* **2004**, *126* (1), 62–63.

(20) Liu, H.; Feng, L.; Zhai, J.; Jiang, L.; Zhu, D. Reversible Wettability of a Chemical Vapor Deposition Prepared ZnO Film between Superhydrophobicity and Superhydrophilicity. *Langmuir* **2004**, *20* (14), 5659–5661.

(21) Chi, P. W.; Su, C. W.; Wei, D. H. Control of Hydrophobic Surface and Wetting States in Ultra-Flat ZnO Films by GLAD Method. *Appl. Surf. Sci.* **2017**, *404*, 380–387.

(22) Fukushima, H.; Uchida, H.; Funakubo, H.; Katoda, T.; Nishida, K. Evaluation of Oxygen Vacancies in ZnO Single Crystals and

Powders by Micro-Raman Spectroscopy. *J. Ceram. Soc. Jpn.* **2017**, *125* (6), 445–448.

(23) Velayi, E.; Norouzebeigi, R. Synthesis of Hierarchical Superhydrophobic Zinc Oxide Nano-Structures for Oil/Water Separation. *Ceram. Int.* **2018**, *44* (12), 14202–14208.

(24) Xu, X.; Chen, D.; Yi, Z.; Jiang, M.; Wang, L.; Zhou, Z.; Fan, X.; Wang, Y.; Hui, D. Antimicrobial Mechanism Based on H₂O₂ Generation at Oxygen Vacancies in ZnO Crystals. *Langmuir* **2013**, *29* (18), 5573–5580.

(25) Polydorou, E.; Zeniou, A.; Tsikritzis, D.; Soultati, A.; Sakellis, I.; Gardelis, S.; Papadopoulos, T. A.; Briscoe, J.; Palilis, L. C.; Kennou, S.; et al. Surface Passivation Effect by Fluorine Plasma Treatment on ZnO for Efficiency and Lifetime Improvement of Inverted Polymer Solar Cells. *J. Mater. Chem. A* **2016**, *4* (30), 11844–11858.

(26) Lee, H. B.; Ginting, R. T.; Tan, S. T.; Tan, C. H.; Alshanaheh, A.; Oleiwi, H. F.; Yap, C. C.; Jumali, M. H. H.; Yahaya, M. Controlled Defects of Fluorine-Incorporated ZnO Nanorods for Photovoltaic Enhancement. *Sci. Rep.* **2016**, *6*, 32645.

(27) Chen, C.; He, H.; Lu, Y.; Wu, K.; Ye, Z. Surface Passivation Effect on the Photoluminescence of ZnO Nanorods. *ACS Appl. Mater. Interfaces* **2013**, *5* (13), 6354–6359.

(28) Choi, J.; Kim, Y.; Jo, J. W.; Kim, J.; Sun, B.; Walters, G.; García de Arquer, F. P.; Quintero-Bermudez, R.; Li, Y.; Tan, C. S.; et al. Chloride Passivation of ZnO Electrodes Improves Charge Extraction in Colloidal Quantum Dot Photovoltaics. *Adv. Mater.* **2017**, *29* (33), 1702350.

(29) Xiao, X.; Cao, G.; Chen, F.; Tang, Y.; Liu, X.; Xu, W. Durable Superhydrophobic Wool Fabrics Coating with Nanoscale Al₂O₃ Layer by Atomic Layer Deposition. *Appl. Surf. Sci.* **2015**, *349*, 876–879.

(30) Chen, Y. C.; Lin, C. H.; Guo, T. F.; Wen, T. C. Surfactant-Enriched ZnO Surface via Sol-Gel Process for the Efficient Inverted Polymer Solar Cell. *ACS Appl. Mater. Interfaces* **2018**, *10* (31), 26805–26811.

(31) Rackauskas, S.; Mustonen, K.; Järvinen, T.; Mattila, M.; Klimova, O.; Jiang, H.; Tolochko, O.; Lipsanen, H.; Kauppinen, E. I.; Nasibulin, A. G. Synthesis of ZnO Tetrapods for Flexible and Transparent UV Sensors. *Nanotechnology* **2012**, *23* (9), 095502.

(32) Newton, M. C.; Firth, S.; Matsuura, T.; Warburton, P. A. Synthesis and Characterisation of Zinc Oxide Tetrapod Nanocrystals. In *Journal of Physics: Conference Series*; Institute of Physics Publishing, 2006; Vol. 26, pp 251–255. DOI: 10.1088/1742-6596/26/1/060.

(33) Zanotti, L.; Calestani, D.; Villani, M.; Zha, M.; Zappettini, A.; Paorici, C. Vapour-Phase Growth, Purification and Large-Area Deposition of ZnO Tetrapod Nanostructures. *Cryst. Res. Technol.* **2010**, *45* (6), 667–671.

(34) Spencer, M. J. S.; Wong, K. W. J.; Yarovsky, I. Surface Defects on ZnO Nanowires: Implications for Design of Sensors. *J. Phys.: Condens. Matter* **2012**, *24* (30), 305001.

(35) Smazna, D.; Shree, S.; Polonskyi, O.; Lamaka, S.; Baum, M.; Zheludkevich, M.; Faupel, F.; Adelung, R.; Mishra, Y. K. Mutual Interplay of ZnO Micro- and Nanowires and Methylene Blue during Cyclic Photocatalysis Process. *J. Environ. Chem. Eng.* **2019**, *7* (2), 103016.

(36) Kaps, S.; Bhowmick, S.; Gröttrup, J.; Hrkac, V.; Stauffer, D.; Guo, H.; Warren, O. L.; Adam, J.; Kienle, L.; Minor, A. M.; et al. Piezoresistive Response of Quasi-One-Dimensional ZnO Nanowires Using an in Situ Electromechanical Device. *ACS Omega* **2017**, *2* (6), 2985–2993.

(37) Vallejos, S.; Gràcia, I.; Pizúrová, N.; Figueras, E.; Cechal, J.; Hubálek, J.; Cané, C. Gas Sensitive ZnO Structures with Reduced Humidity-Interference. *Sens. Actuators, B* **2019**, *301*, 127054.

(38) Huang, A.; Kan, C. C.; Lo, S. C.; Chen, L. H.; Su, D. Y.; Soesanto, J. F.; Hsu, C. C.; Tsai, F. Y.; Tung, K. L. Nanoarchitected Design of Porous ZnO@copper Membranes Enabled by Atomic-Layer-Deposition for Oil/Water Separation. *J. Membr. Sci.* **2019**, *582*, 120–131.

(39) Sharma, M.; Joshi, M.; Nigam, S.; Avasthi, D. K.; Adelung, R.; Srivastava, S. K.; Mishra, Y. K. Efficient Oil Removal from Wastewater

Based on Polymer Coated Superhydrophobic Tetrapodal Magnetic Nanocomposite Adsorbent. *Appl. Mater. Today* **2019**, *17*, 130–141.

(40) Yue, X.; Zhang, T.; Yang, D.; Qiu, F.; Zhu, Y.; Fang, J. In Situ Fabrication Dynamic Carbon Fabrics Membrane with Tunable Wettability for Selective Oil–Water Separation. *J. Ind. Eng. Chem.* **2018**, *61*, 188–196.

(41) Pan, T.; Liu, J.; Deng, N.; Li, Z.; Wang, L.; Xia, Z.; Fan, J.; Liu, Y. ZnO Nanowires@PVDF Nanofiber Membrane with Superhydrophobicity for Enhanced Anti-Wetting and Anti-Scaling Properties in Membrane Distillation. *J. Membr. Sci.* **2021**, *621*, 118877.

(42) Wang, M.; Liu, G.; Yu, H.; Lee, S. H.; Wang, L.; Zheng, J.; Wang, T.; Yun, Y.; Lee, J. K. ZnO Nanorod Array Modified PVDF Membrane with Superhydrophobic Surface for Vacuum Membrane Distillation Application. *ACS Appl. Mater. Interfaces* **2018**, *10* (16), 13452–13461.

(43) Raturi, P.; Singh, J. P. An Intelligent Dual Mode Filtration Device for Separation of Immiscible Oil/Water Mixtures and Emulsions. *Appl. Surf. Sci.* **2019**, *484*, 97–104.

(44) Selim, M. S.; Yang, H.; Wang, F. Q.; Fathallah, N. A.; Huang, Y.; Kuga, S. Silicone/ZnO Nanorod Composite Coating as a Marine Antifouling Surface. *Appl. Surf. Sci.* **2019**, *466*, 40–50.

(45) Wang, M.; Yu, W.; Zhang, Y.; Woo, J. Y.; Chen, Y.; Wang, B.; Yun, Y.; Liu, G.; Lee, J. K.; Wang, L. A Novel Flexible Micro-Ratchet/ZnO Nano-Rods Surface with Rapid Recovery Icephobic Performance. *J. Ind. Eng. Chem.* **2018**, *62*, 52–57.

(46) Chen, X.; Wang, P.; Zhang, D. Designing a Superhydrophobic Surface for Enhanced Atmospheric Corrosion Resistance Based on Coalescence-Induced Droplet Jumping Behavior. *ACS Appl. Mater. Interfaces* **2019**, *11* (41), 38276–38284.

(47) Wang, S.; Li, D.; Zhou, Y.; Jiang, L. Hierarchical Ti₃C₂TxMXene/Ni Chain/ZnO Array Hybrid Nanostructures on Cotton Fabric for Durable Self-Cleaning and Enhanced Microwave Absorption. *ACS Nano* **2020**, *14* (7), 8634–8645.

(48) Rackauskas, S.; Barbero, N.; Barolo, C.; Viscardi, G. ZnO Nanowires for Dye Sensitized Solar Cells. In *Nanowires - New Insights*; InTech, 2017. DOI: 10.5772/67616.

(49) Palamà, I. E.; D'Amone, S.; Biasucci, M.; Gigli, G.; Cortese, B. Bioinspired Design of a Photoresponsive Superhydrophobic/Oleophilic Surface with Underwater Superoleophobic Efficacy. *J. Mater. Chem. A* **2014**, *2* (41), 17666–17675.

(50) Gurav, A. B.; Latthe, S. S.; Vhatkar, R. S.; Lee, J. G.; Kim, D. Y.; Park, J. J.; Yoon, S. S. Superhydrophobic Surface Decorated with Vertical ZnO Nanorods Modified by Stearic Acid. *Ceram. Int.* **2014**, *40* (5), 7151–7160.

(51) Banik, M.; Chakrabarty, P.; Das, A.; Ray, S. K.; Mukherjee, R. Colloidal Transfer Printing-Mediated Fabrication of Zinc Oxide Nanorods for Self-Cleaning Applications. *Adv. Mater. Interfaces* **2019**, *6* (9), 1900063.

(52) Zhou, X.; Wang, G.; Wang, M.; Zhang, Y.; Yin, W.; He, Q. A Simple Preparation Method for Superhydrophobic Surface on Silicon Rubber and Its Properties. *Prog. Org. Coat.* **2020**, *143*, 105612.

(53) Yuan, Y.; Duan, Y.; Zuo, Z.; Yang, L.; Liao, R. Novel, Stable and Durable Superhydrophobic Film on Glass Prepared by RF Magnetron Sputtering. *Mater. Lett.* **2017**, *199*, 97–100.

(54) Milonias, A.; Tripathy, A.; Donati, M.; Sharma, C. S.; Pan, F.; Maniura-Weber, K.; Ren, Q.; Poulikakos, D. Water-Based Scalable Methods for Self-Cleaning Antibacterial ZnO-Nanostructured Surfaces. *Ind. Eng. Chem. Res.* **2020**, *59* (32), 14323–14333.

(55) Velayi, E.; Norouzebeigi, R. Single-Step Prepared Hybrid ZnO/CuO Nanopowders for Water Repellent and Corrosion Resistant Coatings. *Ceram. Int.* **2019**, *45* (14), 16864–16872.

(56) Jin, X.; Deng, M.; Kaps, S.; Zhu, X.; Holken, I.; Mess, K.; Adelung, R.; Mishra, Y. K. Study of Tetrapodal ZnO-Pdms Composites: A Comparison of Fillers Shapes in Stiffness and Hydrophobicity Improvements. *PLoS One* **2014**, *9* (9), No. e106991.

(57) Fragalà, M. E.; Di Mauro, A.; Cristaldi, D. A.; Cantarella, M.; Impellizzeri, G.; Privitera, V. ZnO Nanorods Grown on Ultrathin ZnO Seed Layers: Application in Water Treatment. *J. Photochem. Photobiol., A* **2017**, *332*, 497–504.

- (58) Das, S.; Meena, S. S.; Pramanik, A. Zinc Oxide Functionalized Human Hair: A Potential Water Decontaminating Agent. *J. Colloid Interface Sci.* **2016**, *462*, 307–314.
- (59) Buasakun, J.; Srilaong, P.; Chaloeipote, G.; Rattanakram, R.; Wongchoosuk, C.; Duangthongyou, T. Synergistic Effect of ZnO/ZIF8 Heterostructure Material in Photodegradation of Methylene Blue and Volatile Organic Compounds with Sensor Operating at Room Temperature. *J. Solid State Chem.* **2020**, *289*, 121494.
- (60) Sharma, M.; Poddar, M.; Gupta, Y.; Nigam, S.; Avasthi, D. K.; Adelung, R.; Abolhassani, R.; Fiutowski, J.; Joshi, M.; Mishra, Y. K. Solar Light Assisted Degradation of Dyes and Adsorption of Heavy Metal Ions from Water by CuO–ZnO Tetrapodal Hybrid Nanocomposite. *Mater. Today Chem.* **2020**, *17*, 100336.
- (61) Thirumalai, K.; Balachandran, S.; Swaminathan, M. Superior Photocatalytic, Electrocatalytic, and Self-Cleaning Applications of Fly Ash Supported ZnO Nanorods. *Mater. Chem. Phys.* **2016**, *183*, 191–200.
- (62) Gao, X.; Wen, G.; Guo, Z. Durable Superhydrophobic and Underwater Superoleophobic Cotton Fabrics Growing Zinc Oxide Nanoarrays for Application in Separation of Heavy/Light Oil and Water Mixtures as Need. *Colloids Surf., A* **2018**, *559*, 115–126.
- (63) Raturi, P.; Yadav, K.; Singh, J. P. ZnO-Nanowires-Coated Smart Surface Mesh with Reversible Wettability for Efficient On-Demand Oil/Water Separation. *ACS Appl. Mater. Interfaces* **2017**, *9* (7), 6007–6013.
- (64) Velayi, E.; Norouzbegi, R. A Mesh Membrane Coated with Dual-Scale Superhydrophobic Nano Zinc Oxide: Efficient Oil-Water Separation. *Surf. Coat. Technol.* **2020**, *385*, 125394.
- (65) Bai, X.; Zhao, Z.; Yang, H.; Li, J. ZnO Nanoparticles Coated Mesh with Switchable Wettability for On-Demand Ultrafast Separation of Emulsified Oil/Water Mixtures. *Sep. Purif. Technol.* **2019**, *221*, 294–302.
- (66) Parani, S.; Oluwafemi, O. S. Fabrication of Superhydrophobic Polyethersulfone-ZnO Rods Composite Membrane. *Mater. Lett.* **2020**, *281*, 128663.
- (67) Zhang, W.; Wang, S.; Xiao, Z.; Yu, X.; Liang, C.; Zhang, Y. Frosting Behavior of Superhydrophobic Nanoarrays under Ultralow Temperature. *Langmuir* **2017**, *33* (36), 8891–8898.
- (68) Zuo, Z.; Liao, R.; Zhao, X.; Song, X.; Qiao, Z.; Guo, C.; Zhuang, A.; Yuan, Y. Anti-Frosting Performance of Superhydrophobic Surface with ZnO Nanorods. *Appl. Therm. Eng.* **2017**, *110*, 39–48.
- (69) Liu, G.; Yuan, Y.; Jiang, Z.; Youdong, J.; Liang, W. Anti-Frosting/Anti-Icing Property of Nano-FzO Superhydrophobic Surface on Al Alloy Prepared by Radio Frequency Magnetron Sputtering. *Mater. Res. Express* **2020**, *7* (2), 26401.
- (70) Jiang, S.; Zhang, H.; Jiang, C.; Liu, X. Antifrosting Performance of a Superhydrophobic Surface by Optimizing the Surface Morphology. *Langmuir* **2020**, *36* (34), 10156–10165.
- (71) Liao, R.; Li, C.; Yuan, Y.; Duan, Y.; Zhuang, A. Anti-Icing Performance of ZnO/SiO₂/PTFE Sandwich-Nanostructure Superhydrophobic Film on Glass Prepared via RF Magnetron Sputtering. *Mater. Lett.* **2017**, *206*, 109–112.
- (72) Singh, A.; Singh, S. ZnO Nanowire-Coated Hydrophobic Surfaces for Various Biomedical Applications. *Bull. Mater. Sci.* **2018**, *41*, 94.
- (73) Iqbal, T.; Aziz, A.; Khan, M.A.; Andleeb, S.; Mahmood, H.; Khan, A. A.; Khan, R.; Shafique, M. Surfactant Assisted Synthesis of ZnO Nanostructures Using Atmospheric Pressure Microplasma Electrochemical Process with Antibacterial Applications. *Mater. Sci. Eng., B* **2018**, *228*, 153–159.
- (74) Gao, D.; Liu, J.; Lyu, L.; Li, Y.; Ma, J.; Baig, W. Construct the Multifunction of Cotton Fabric by Synergism between Nano ZnO and Ag. *Fibers Polym.* **2020**, *21* (3), 505–512.
- (75) Gao, D.; Lyu, L.; Lyu, B.; Ma, J.; Yang, L.; Zhang, J. Multifunctional Cotton Fabric Loaded with Ce Doped ZnO Nanorods. *Mater. Res. Bull.* **2017**, *89*, 102–107.
- (76) Mohd Yusof, H.; Mohamad, R.; Zaidan, U. H.; Abdul Rahman, N. A. Microbial Synthesis of Zinc Oxide Nanoparticles and Their Potential Application as an Antimicrobial Agent and a Feed Supplement in Animal Industry: A Review. *Journal of Animal Science and Biotechnology* **2019**, *10*, 57 DOI: 10.1186/s40104-019-0368-z.
- (77) Bhargav, P. K.; Murthy, K. S. R.; Pandey, J. K.; Mandal, P.; Goyat, M. S.; Bhatia, R.; Varanasi, A. Tuning the Structural, Morphological, Optical, Wetting Properties and Anti-Fungal Activity of ZnO Nanoparticles by C Doping. *Nano-Structures and Nano-Objects* **2019**, *19*, 100365.
- (78) Papavlassopoulos, H.; Mishra, Y. K.; Kaps, S.; Paulowicz, L.; Abdelaziz, R.; Elbahri, M.; Maser, E.; Adelung, R.; Röhl, C. Toxicity of Functional Nano-Micro Zinc Oxide Tetrapods: Impact of Cell Culture Conditions, Cellular Age and Material Properties. *PLoS One* **2014**, *9* (1), No. e84983.
- (79) Tereshchenko, A.; Yazdi, G. R.; Konup, I.; Smytyna, V.; Khranovskyy, V.; Yakimova, R.; Ramanavicius, A. Application of ZnO Nanorods Based Whispering Gallery Mode Resonator in Optical Immunosensors. *Colloids Surf., B* **2020**, *191*, 110999.
- (80) Madhu, S.; Anthuvan, A. J.; Ramasamy, S.; Manickam, P.; Bhansali, S.; Nagamony, P.; Chinnuswamy, V. ZnO Nanorod Integrated Flexible Carbon Fibers for Sweat Cortisol Detection. *ACS Appl. Electron. Mater.* **2020**, *2* (2), 499–509.
- (81) Hen, M.; Edri, E.; Guy, O.; Avrahami, D.; Shpaysman, H.; Gerber, D.; Sukenik, C. N. Microfluidic Devices Containing ZnO Nanorods with Tunable Surface Chemistry and Wetting-Independent Water Mobility. *Langmuir* **2019**, *35* (9), 3265–3271.
- (82) Prasad, M. D.; Shaik, U. P.; Madhurima, V.; Krishna, M. G. Low Temperature Growth of ZnO Nanostructures on Flexible Polystyrene Substrates for Optical, Photoluminescence and Wettability Applications. *Mater. Res. Express* **2016**, *3* (8), 085010.
- (83) Mueen, R.; Lerch, M.; Cheng, Z.; Konstantinov, K. Na-Doped ZnO UV Filters with Reduced Photocatalytic Activity for Sunscreen Applications. *J. Mater. Sci.* **2020**, *55* (7), 2772–2786.
- (84) Nguyen, N. T.; Nguyen, T. M. N.; Le, N. T.; Le, T. K. Suppressing the Photocatalytic Activity of ZnO Nanoparticles by Al-Doping for the Application in Sunscreen Products. *Mater. Technol.* **2020**, *35* (6), 349–355.
- (85) Vieira, C. O.; Grice, J. E.; Roberts, M. S.; Haridass, I. N.; Duque, M. D.; Lopes, P. S.; Leite-Silva, V. R.; Martins, T. S. ZnO:SBA-15 Nanocomposites for Potential Use in Sunscreen: Preparation, Properties, Human Skin Penetration and Toxicity. *Skin Pharmacol. Physiol.* **2018**, *32* (1), 32–42.
- (86) Balanand, S.; Maria, M. J.; Rajan, T. P. D.; Peer Mohamed, A.; Ananthakumar, S. Bulk Processing of ZnO Nanostructures via Microwave Assisted Oxidation of Mechanically Seeded Zn Dust for Functional Paints and Coatings. *Chem. Eng. J.* **2016**, *284*, 657–667.
- (87) Li, C.; Chen, Y.; Wang, P.; Wang, G.; Cheng, Q.; Ou, J.; Zhang, D. Dynamic Self-Propelling Condensed Microdroplets over Super-Hydrophobic Surface: An Exceptional Atmospheric Corrosion Inhibition Strategy. *Colloids Surf., A* **2021**, *613*, 126055.
- (88) Selim, M. S.; El-Safty, S. A.; Abbas, M. A.; Shenashen, M. A. Facile Design of Graphene Oxide-ZnO Nanorod-Based Ternary Nanocomposite as a Superhydrophobic and Corrosion-Barrier Coating. *Colloids Surf., A* **2021**, *611*, 125793.
- (89) Weththimuni, M. L.; Capsoni, D.; Malagodi, M.; Licchelli, M. Improving Wood Resistance to Decay by Nanostructured ZnO-Based Treatments. *J. Nanomater.* **2019**, *2019*, 6715756.
- (90) Shaban, M.; Zayed, M.; Hamdy, H. Nanostructured ZnO Thin Films for Self-Cleaning Applications. *RSC Adv.* **2017**, *7* (2), 617–631.
- (91) Truong, N. T. N.; Hoang, H. H. T.; Park, C. Improvement of Vacuum Free Hybrid Photovoltaic Performance Based on a Well-Aligned ZnO Nanorod and WO₃ as a Carrier Transport Layer. *Materials* **2019**, *12* (9), 1490.
- (92) Pandiyarasan, V.; Suhasini, S.; Archana, J.; Navaneethan, M.; Majumdar, A.; Hayakawa, Y.; Ikeda, H. Fabrication of Hierarchical ZnO Nanostructures on Cotton Fabric for Wearable Device Applications. *Appl. Surf. Sci.* **2017**, *418*, 352–361.
- (93) Utari, L.; Septiani, N. L. W.; Suyatman; Nugraha; Nur, L. O.; Wasisto, H. S.; Yulianto, B. Wearable Carbon Monoxide Sensors Based on Hybrid Graphene/ZnO Nanocomposites. *IEEE Access* **2020**, *8*, 49169–49179.

(94) Subbiah, D. K.; Mani, G. K.; Babu, K. J.; Das, A.; Balaguru Rayappan, J. B. Nanostructured ZnO on Cotton Fabrics – A Novel Flexible Gas Sensor & UV Filter. *J. Cleaner Prod.* **2018**, *194*, 372–382.

(95) Gu, P.; Zhu, X.; Yang, D. Vertically Aligned ZnO Nanorods Arrays Grown by Chemical Bath Deposition for Ultraviolet Photodetectors with High Response Performance. *J. Alloys Compd.* **2020**, *815*, 152346.

(96) Abdulrahman, A. F.; Ahmed, S. M.; Barzinjy, A. A.; Hamad, S. M.; Ahmed, N. M.; Almessiere, M. A. Fabrication and Characterization of High-Quality UV Photodetectors Based ZnO Nanorods Using Traditional and Modified Chemical Bath Deposition Methods. *Nanomaterials* **2021**, *11* (3), 677.

(97) Ajmal, H. M. S.; Khan, F.; Huda, N. U.; Lee, S.; Nam, K.; Kim, H. Y.; Eom, T.-H.; Kim, S. D. High-Performance Flexible Ultraviolet Photodetectors with Ni/Cu-Codoped ZnO Nanorods Grown on PET Substrates. *Nanomaterials* **2019**, *9* (8), 1067.

(98) Ajmal, H. M. S.; Khan, F.; Nam, K.; Kim, H. Y.; Kim, S. D. Ultraviolet Photodetection Based on High-Performance Co-plus-Ni Doped ZnO Nanorods Grown by Hydrothermal Method on Transparent Plastic Substrate. *Nanomaterials* **2020**, *10* (6), 1225.

(99) Abdalla, J. T.; Jiao, S.; Wang, D.; Zeng, Z.; Zhang, B.; Guichard, H.; Wang, J. Enhanced Ag@SnO₂ Plasmonic Nanoparticles for Boosting Photoluminescence and Photocurrent Response of ZnO Nanorod UV Photodetectors. *J. Electron. Mater.* **2020**, *49* (9), 5657–5665.

(100) Huang, C. Y.; Kang, C. C.; Ma, Y. C.; Chou, Y. C.; Ye, J. H.; Huang, R. T.; Siao, C. Z.; Lin, Y. C.; Chang, Y. H.; Shen, J. L.; et al. P-GaN/n-ZnO Nanorods: The Use of Graphene Nanosheets Composites to Increase Charge Separation in Self-Powered Visible-Blind UV Photodetectors. *Nanotechnology* **2018**, *29* (44), 445201.

(101) Fu, Q.-M.; Yao, Z.-C.; Peng, J.-L.; Zhao, H.-Y.; Ma, Z.-B.; Tao, H.; Tu, Y.-F.; Zhou, D.; Tian, Y. Enhanced Photoresponse in ZnO Nanorod Array/p-GaN Self-Powered Ultraviolet Photodetectors via Coupling with CuO Nanostructures. *Mater. Res. Express* **2020**, *7* (1), 015063.

(102) Zarezadeh, E.; Ghorbani, A. Bipolar Photoresponse Ultraviolet Photodetectors Based on ZnO Nanowires. *Mater. Res. Express* **2020**, *7* (5), 056203.